Proton glassy behavior in $Rb_{1-x}(NH_4)_xH_2AsO_4$ mixed crystal

Sangbo Kim and Sook-Il Kwun
Department of Physics, Seoul National University, Seoul 151-742, Korea
(Received 16 October 1989; revised manuscript received 23 January 1990)

The mixed crystal $Rb_{1-x}(NH_4)_xH_2AsO_4$ of ferroelectric RbH_2AsO_4 and antiferroelectric $NH_4H_2AsO_4$ has been investigated for several values of x by measuring the dielectric constant along the a and c axis in the temperature range from 30 to 200 K. The phase boundary between the ferroelectric phase and the proton glass state is found to be between 0.13 and 0.20, and a similar boundary between the proton glass state and the antiferroelectric phase is observed to be located between 0.44 and 0.49. For samples with $0.23 \le x \le 0.44$, the dielectric data can be scaled using the Vogel-Fulcher law with a static freezing temperature T_0. From our experimental results, we construct a phase diagram of $Rb_{1-x}(NH_4)_xH_2AsO_4$.

I. INTRODUCTION

The phase diagram of the $Rb_{1-x}(NH_4)_xH_2PO_4$ (abbreviated as RADP) mixed crystal has been investigated by Courtens[1,2] in the Rb-rich region and by Iida and Terauchi[3] on the NH_4-rich side. In the small ($x<0.22$) or large ($x>0.78$) concentration range RADP undergoes a transition to the ferroelectric (FE) or antiferroelectric (AFE) phase, respectively. The phase diagram of RADP is almost symmetric[4,5] since the transition temperatures of RbH_2PO_4 (abbreviated as RDP) and $NH_4H_2PO_4$ (abbreviated as ADP) are nearly the same. In the intermediate ($0.22 \le x \le 0.78$) concentration range, the frequency-dependent susceptibility cusp was seen at low temperatures. Courtens showed that the entire imaginary dielectric constant (ϵ'') data could fall onto a single curve with two fitting parameters using the Vogel-Fulcher law.[6-8] Moreover, Raman and Brillouin scattering measurements also support these fitting parameters of the Vogel-Fulcher law.[9,10]

Following the investigations on the RADP mixed crystal, the mixed $Rb_{1-x}(NH_4)_xH_2AsO_4$ (abbreviated as RADA) crystal of ferroelectric RbH_2AsO_4 (RDA, $T_c=110$ K) and antiferroelectric $NH_4H_2AsO_4$ (ADA, $T_N=216$ K) has been studied. Similar to the RADP system, the structure and lattice constants[11] of RDA and ADA are nearly the same. So the mixed crystals can be obtained over the full range of x, $0 \le x \le 1$. However, in contrast to the RADP system in which it has $T_c \approx T_N$, the RADA system has a large difference between the two transition temperatures; $T_N \approx 2T_c$. In the case of RADA, it is expected that the phase diagram is rather asymmetric because of this large difference between the transition temperatures of RDA and ADA. Recently, Trybula *et al.* reported dielectric constant measurements on the RADA system at a microwave frequency.[12] They reported glasslike behaviors for samples with $0.1<x<0.5$.

In this paper we report the dielectric constant measurement on several samples of the RADA system and its phase diagram. We show the detailed dielectric response data particularly for the proton glass state samples, i.e., $0.23 \le x \le 0.44$. The imaginary part of dielectric constant for these samples can be explained by the scaling formula based on a Vogel-Fulcher law just like the RADP system.

II. EXPERIMENTS

The pure RDA and ADA powders were obtained by reacting rubidium carbonate and ammonium carbonate, respectively, with an arsenic acid solution. The resulting carbonic acid was discomposed into CO_2 gas and water by heating the solution. After filtering off the insoluble impurities, the solution was evaporated for crystallization. Then we mixed RDA and ADA powders into distilled water with proper weight fractions. Using a slow evaporation method, we obtained the $Rb_{1-x}(NH_4)_xH_2AsO_4$ mixed crystals. The concentrations (x) of our samples were determined by a titration method.

The RADA mixed crystals were cut into platelet form using a thread saw. After being polished, the sample faces were coated with solver by vacuum evaporation to serve as electrodes. Both the capacitances and conductances were measured simultaneously by an impedance analyzer (Hewlett Packard 4192A) at temperatures between 30 and 200 K. A closed-cycle helium-refrigerator cell (CTI) was used to control the temperature.

III. RESULTS AND DISCUSSION

Since the ferroelectric axis of RDA is the c axis, the dielectric constant measurement along c axis is essential to determine whether the RADA with a certain value of x will have a ferroelectric phase transition. We measured the real (ϵ_c') and imaginary (ϵ_c'') parts of the dielectric constants along the c axis for various values of x at 1 MHz as a function of temperature. The ϵ_c' data are shown in Fig. 1. As shown in Fig. 1(a), ϵ_c' along the c axis for the $x=0.08$ and 0.13 samples show cusps, characteristic behaviors of ϵ_c' at the ferroelectric phase transi-

tion, at 105 and 89 K, respectively. These curves are well fitted to the Curie-Weiss law above the cusp temperatures. This experimental observation shows that the ferroelectric phase transition occurs for the $x=0.08$ and 0.13 samples. The imaginary dielectric constant curves also support the fact that these samples undergo the ferroelectric transition in agreement with the recent birefringence measurement.[13]

Since changes of ϵ_c' at 1 MHz for $x \geq 0.20$ samples become small, we lowered our measurement frequency to 10 kHz. The temperature dependence of the dielectric constants at 10 kHz is shown in Fig. 1(b). The temperature at which the maximum of ϵ_c' occurs is getting lower as x increases, just like in the ferroelectric phase region. However, compared to Fig. 1(a), ϵ_c' for the samples with $x=0.20$, 0.23, and 0.37 do not show the cusps. Moreover, ϵ_c' and ϵ_c'' are dependent on the frequency around the onset temperature, as discussed later in this paper. All of these behaviors clearly indicate that the samples with $x=0.20$, 0.23, and 0.37 show glassy behaviors. Therefore, the phase boundary between ferroelectric phase and glass state is expected to be located at $0.13 < x < 0.20$.

Since the ADA crystal has an antiferroelectric phase along the a axis below a critical temperature, the dielectric constant measurement along the a axis will provide a criterion for determining the phase boundary between the glass state and the antiferroelectric phase. In Fig. 2(a), the ϵ_a' data along the a axis for the $x=0.20$ and 0.44 samples at 10 kHz are shown. These data show broad peaks instead of cusps. Moreover, the temperature dependence of ϵ_a' for these samples above the peak temperature deviates from the Curie-Weiss law indicating that these samples belong to the glass state.

Figure 2(b) shows the temperature dependences of ϵ_a' along the a axis for the $x=0.49$, 0.70, and 0.75 samples at 1 MHz. Samples with $x=0.70$ and 0.75 show a discontinuous anomaly in ϵ_a', characteristics of an antiferroelectric transition, at 122 and 151 K, respectively. The sample with $x=0.49$ shows a rather broader peak in ϵ_a' than those for $x \geq 0.70$ samples, but the ϵ_a' data follow

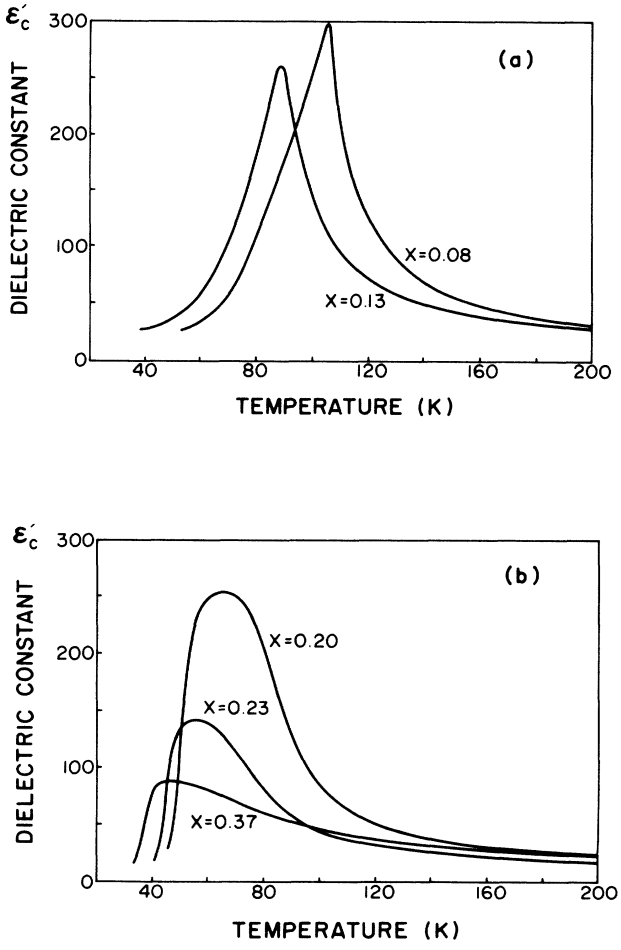

FIG. 1. The real part (ϵ_c') of the dielectric constant of $Rb_{1-x}(NH_4)_xH_2AsO_4$ along the c axis. (a) The samples with $x=0.08$ and 0.13 are measured at 1 MHz. (b) The samples with $x=0.20$, 0.23, and 0.37 are measured at 10 kHz.

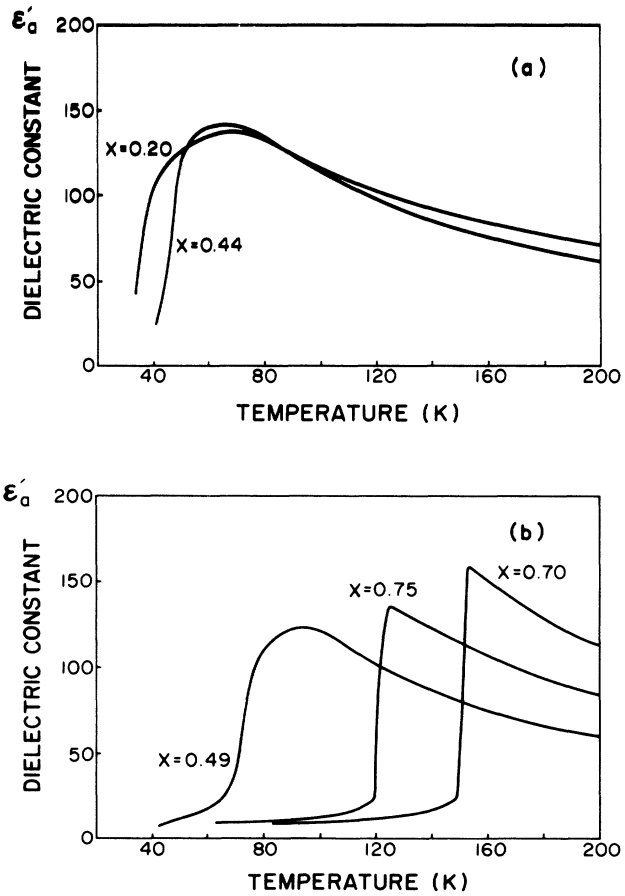

FIG. 2. The real part (ϵ_a') of the dielectric constant of $Rb_{1-x}(NH_4)_xH_2AsO_4$ along the a axis. (a) The samples with $x=0.20$ and 0.44 are measured at 10 kHz. (b) The samples with $x=0.49$, 0.70, and 0.75 are measured at 1 MHz.

the Curie-Weiss law above 96 K. Moreover, ϵ_a'' data for the $x=0.49$ sample are nearly temperature independent and do not show the dispersion, which is the characteristic of the glass state. Therefore, the phase boundary between the proton glass state and the antiferroelectric phase will be located at $0.44<x<0.49$.

Changes in ϵ_a' between the $x=0.49$ and 0.70 samples, as shown in Fig. 2(b), indicate that the RADA system should have a changeover from a second-order to a first-order phase transition between these two concentrations of x. According to Courtens,[2] a similar changeover was observed in the RADP system between $x=0.1$ and 0.2. In the case of the $x=0.49$ sample, the transition temperature is determined to be 72 K, i.e., the temperature at which ϵ_a' has the mean value between its peak and low value.[14]

On the problem of the order-parameter anisotropy, Kim *et al.* reported that ϵ_a' showed no peak down to 20 K for their sample of $x=0.35$ (RADA) while ϵ_c' showed a glass transition with the onset at 42 K.[15] In our dielectric constant measurement for $x=0.37$, we do not observe the above phenomena but observe that both ϵ_a' and ϵ_c' have the onset temperature below which ϵ' starts to decrease. We also find a small difference between the on-

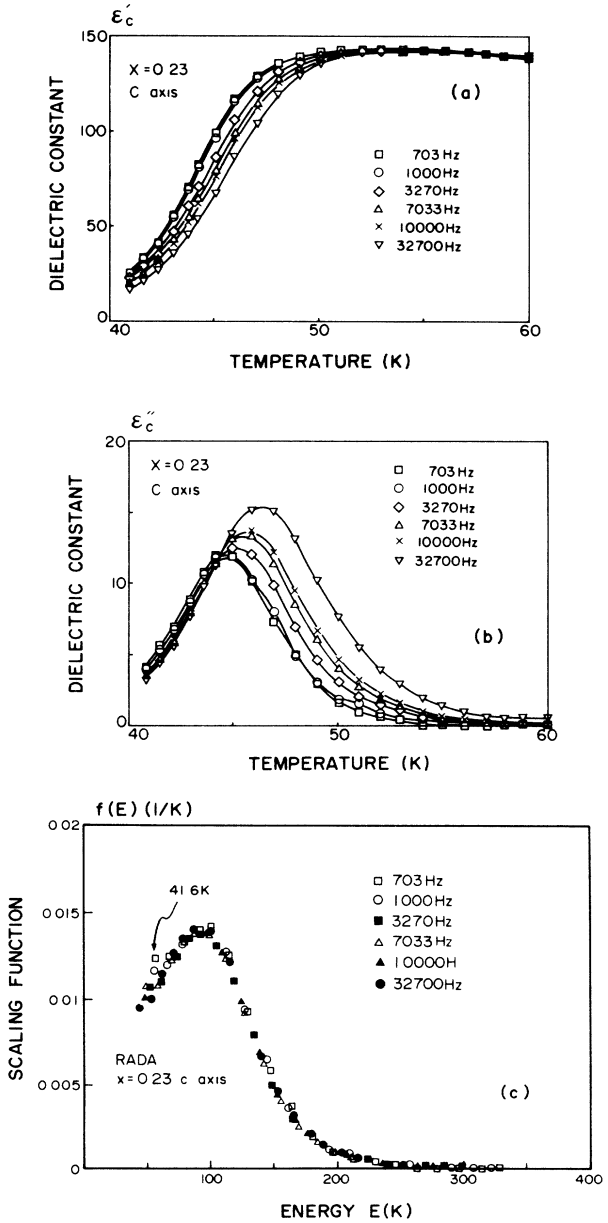

FIG. 3. The dielectric constant of the c-cut sample of RADA for $x=0.23$. The thin lines are to guide the eyes. (a) ϵ_c' vs the temperature. (b) ϵ_c'' vs the temperature. (c) The scaling function vs the energy variable.

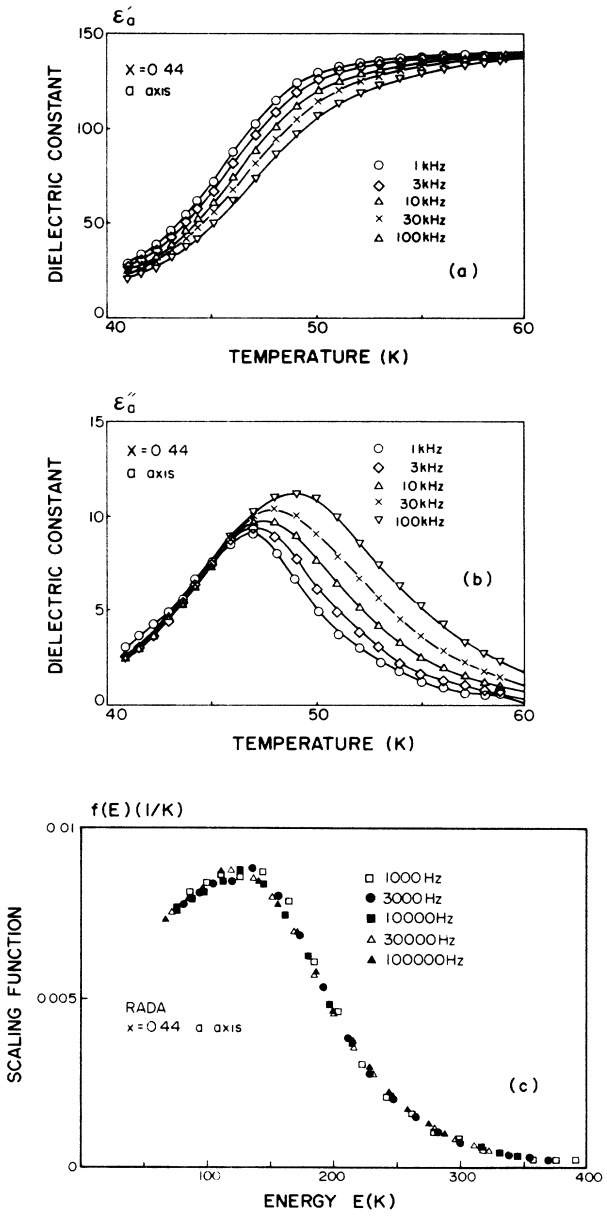

FIG. 4. The dielectric constant of the a-cut sample of RADA for $x=0.44$. The thin lines are to guide the eyes. (a) ϵ_a' vs the temperature. (b) ϵ_a'' vs the temperature. (c) The scaling function vs the energy variable.

set temperatures of the a-cut and c-cut samples as was reported by Trybula *et al.*[16]

To investigate the glassy behavior of the RADA system, we measured ϵ' and ϵ'' for $0.23 \leq x \leq 0.44$ samples in various frequencies between 700 Hz and 32.7 kHz. (Because of the small size of our sample, a measurement at lower frequency below 700 Hz does not give enough resolution.) In the proton glass state, there should be dependence of ϵ' and ϵ'' on the frequency, i.e., there should exist a dispersion of ϵ' and ϵ''. The ϵ_c' data along the c axis for the $x=0.23$ sample are shown in Fig. 3(a). In these low frequencies, the peak structure observed in ϵ' of either the ferroelectric or antiferroelectric phase cannot be observed in this sample. Moreover, as the frequency becomes higher, the rolloff region of ϵ_c' also moves to a higher temperature. These kinds of glassy behaviors can be more easily seen in the ϵ_c'' data, as shown in Fig. 3(b). For a given measurement frequency, the ϵ_c'' data show a peak at a temperature which we define as a glass temperature, T_g. Just like the behavior of ϵ_c', T_g moves to a higher temperature as the frequency increases.

One can easily find that the behaviors of our ϵ_c'' curves are very similar to those of the RADP which were observed by Courtens.[6] To explain his ϵ'' data for glassy samples of the RADP system, he suggested the following scaling procedure:

$$\epsilon''(\nu,T) \cong \frac{\pi}{2}(T-T_0)[\epsilon_s(T)-\epsilon_\infty] f((T-T_0)\ln(\nu_0/\nu)) ,$$

assuming a simple distribution of Vogel-Fulcher activation energies.[7] In this scaling form, T_0 is the static freezing temperature and ν_0 is the attempt frequency. The above equation fails below a certain temperature at which the distribution of the relaxation times does not reach its equilibrium value. The temperature range for scaling must be chosen carefully since the scaling parameters (T_0,ν_0) are strongly dependent on this temperature range. Using the ϵ_c'' data between 42 and 58 K, we obtained an excellent scaling behavior which is shown in Fig. 3(c). In this scaling process, $[\epsilon_s(T)-\epsilon_\infty]$ is assumed to be constant, 138. Values for T_0 and $\ln\nu_0$ are obtained to be 38.7 ± 1.0 K and 23.1 ± 1.0 (ν_0 in Hz), respectively. We also present the ϵ_a of RADA for the $x=0.44$ sample in Fig. 4. The values of $[\epsilon_s(T)-\epsilon_\infty]$, T_0, and $\ln\nu_0$ for the $x=0.44$ sample are 133, 38.7 ± 1.0 K, and 26.4 ± 1.0 (ν_0 in Hz), respectively.

These excellent scaling behaviors indicate that a nonzero freezing temperature T_0 can exist in the RADA system just like the RADP and the deuterated RADP systems. It is interesting to note that values of T_0 and $\ln\nu_0$ for the $x=0.44$ sample are close to those of $x=0.62$ sample in the deuterated RADP system but the values of T_0 are larger than those of the RADP system. However, the ν_0 value for the $x=0.23$ sample is to be 11 GHz, which is about 1 order of magnitude smaller than that of the $x=0.44$ sample. This big difference in ν_0 is a very interesting phenomenon and further studies are required to understand this interesting behavior.

Based on our experimental results, the phase diagram of RADA is presented in Fig. 5. Compared to the RADP system, several different features are noticed. The proton glass phase boundary is asymmetric due to the difference between the transition temperature of RDA and that of ADA. The proton glass phase region of the RADA system is narrower than that of the RADP system. The T_g's and T_0's are larger than those of the RADP system. Compared to the RADA phase diagram reported by Trybula *et al*, our phase diagram shows more detailed behaviors in the glass transition region. Moreover, our diagram is based on the audio frequency dielectric constant measurement whereas the phase diagram reported by Trybula *et al.* was constructed by a microwave measurement.

In conclusion, we have demonstrated that the imaginary parts of the dielectric constants for the $0.23 \leq x \leq 0.44$ samples follow the scaling behavior based on the Vogel-Fulcher law with a finite freezing temperature. This scaling behavior indicates that these samples have proton glass states. Based on these experimental findings, we present a revised phase diagram for RADA.

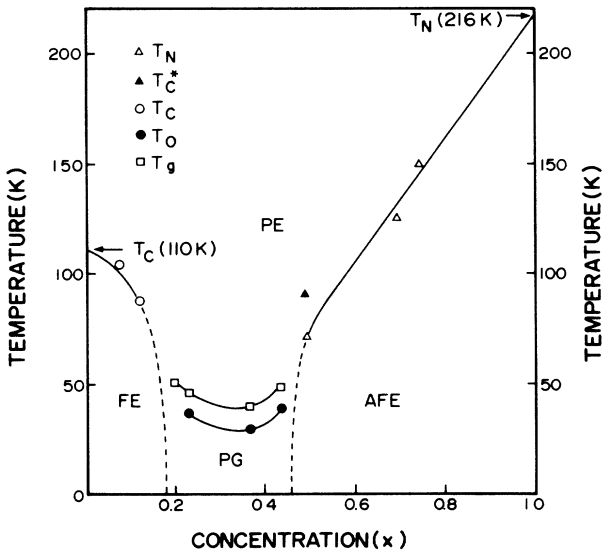

FIG. 5. The phase diagram of $Rb_{1-x}(NH_4)_xH_2AsO_4$ in the T-x plane. The thin lines are phase boundaries. Here T_c^* is the onset temperature of ϵ_a' of the $x=0.49$ sample. We determine AFE boundaries from T_N. The T_g's are chosen where ϵ_a'' at the frequency of 10 kHz has its maximum value. PE: paraelectric phase, PG: proton glass state, FE: ferroelectric phase, AFE: antiferroelectric phase.

ACKNOWLEDGMENTS

The authors are grateful to Professor T.-W. Noh for his valuable comments and to Professor H.-K. Kim for allowing us to use his instruments. The present studies were supported by the Basic Science Research Institute Program, Ministry of Education, Republic of Korea, and Korea Science and Engineering Foundation.

[1]E. Courtens, J. Phys. Lett. (Paris) **43**, L199 (1982).
[2]E. Courtens, Helv. Phys. Acta **56**, 705 (1983).
[3]S. Iida and H. Terauchi, J. Phys. Soc. Jpn. **52**, 4044 (1983).
[4]E. Courtens, Ferroelectrics **72**, 229 (1987).
[5]V. H. Schmidt, Ferroelectrics **72**, 157 (1987).
[6]E. Courtens, Phys. Rev. Lett. **52**, 69 (1984).
[7]E. Courtens, Phys. Rev. B **33**, 2975 (1986).
[8]H. J. Bruckner, E. Courtens, and H. G. Unruh, Z. Phys. B **73**, 337 (1988).
[9]E. Courtens, R. Vacher, and Y. Dagorn, Phys. Rev. B **33**, 7625 (1986).
[10]E. Courtens, R. Vacher, and Y. Dagorn, Phys. Rev. B **36**, 318 (1987).
[11]*Ferro- and Antiferroelectric Substances in Numerical Data and Functional Relationships in Science and Technology* (Springer-Verlag, Berlin, 1969), Vol. **III/3**, p. 143; *Ferro- and Antiferroelectric Substances in Numerical Data and Functional Relationships in Science and Technology* (Springer-Verlag, Berlin, 1975), Vol. **III/9**, p. 138.
[12]Z. Trybula, J. Stankovsky, L. Szczepanska, R. Blinc, Al. Weiss, and N. S. Dalal, Physica B **153**, 143 (1988).
[13]D. Sommer, W. Kleemann, J. G. Yoon, S. I. Kwun, and S. Kim (unpublished).
[14]G. A. Samara, Ferroelectrics **72**, 161 (1987).
[15]J.-J. Kim, N. Kim, and K.-S. Lee, J. Phys. C **21**, L663 (1988).
[16]Z. Trybula, V. H. Schmidt, J. E. Drumheller, D. He, and Z. Li, Phys. Rev. B **40**, 5289 (1989).